Electronic Supplementary Material (ESI) for Organic & Biomolecular Chemistry

Investigating the Effect of Macrocycle Size in Anion Templated Imidazolium-Based Interpenetrated and Interlocked Assemblies

Graeme T. Spence, Nicholas G. White and Paul D. Beer*

Department of Chemistry, University of Oxford,
Mansfield Road, Oxford, OX1 3TA, UK.

Supplementary Information

Part I: Spectral Characterisation of Novel Compounds

Macrocycle **4**

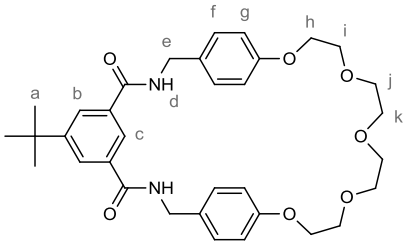

4

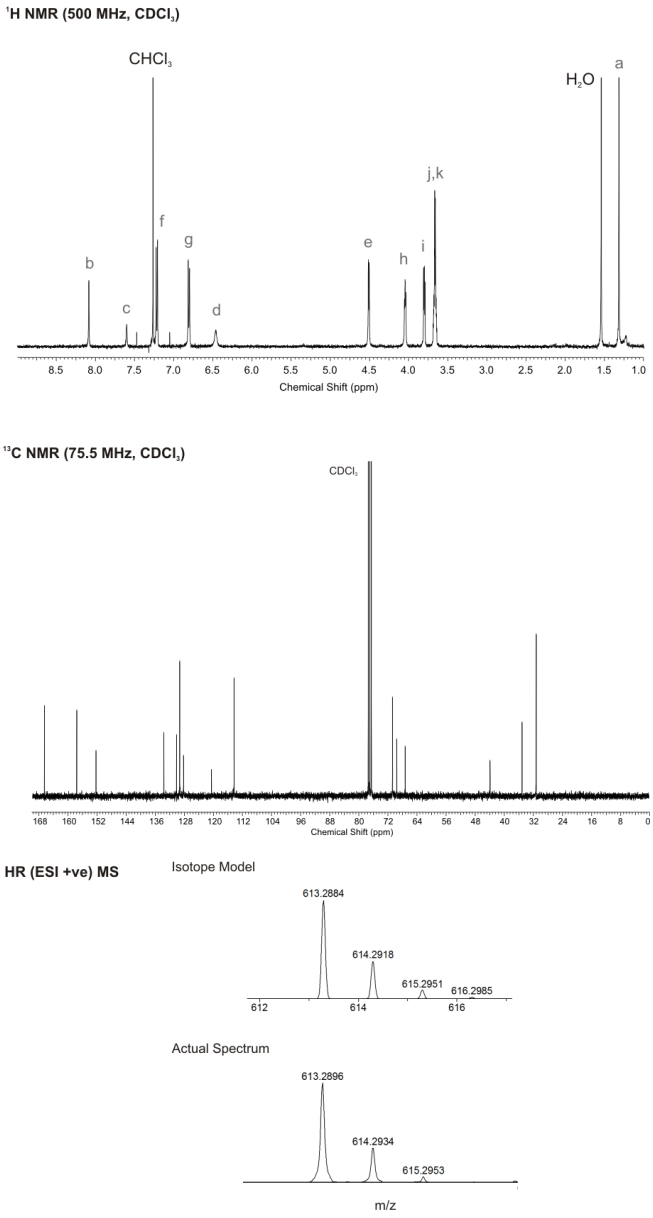

Supplementary Fig. S1 ^{1}H and ^{13}C NMR spectra and high resolution MS of macrocycle **4**.

Rotaxane **8**·Cl

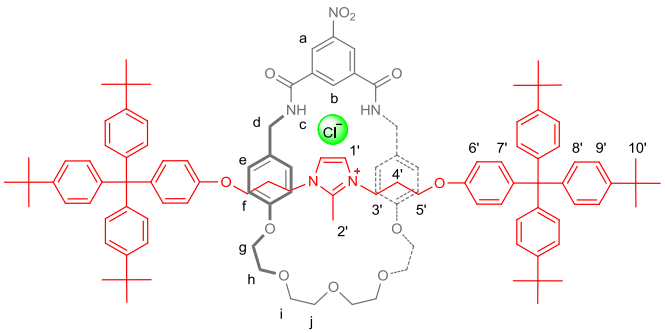

8·Cl

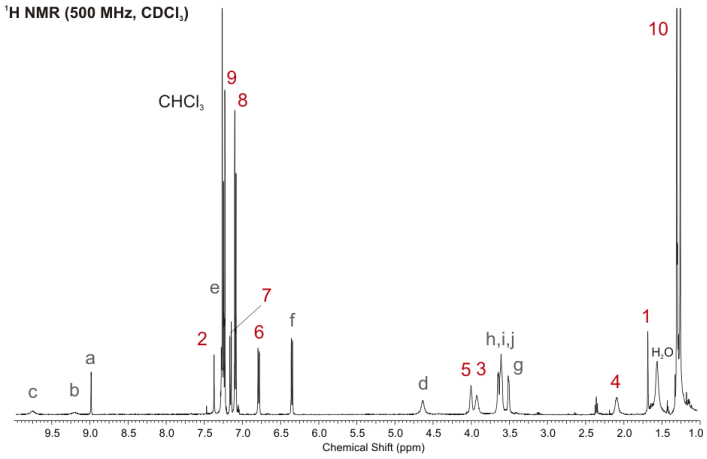

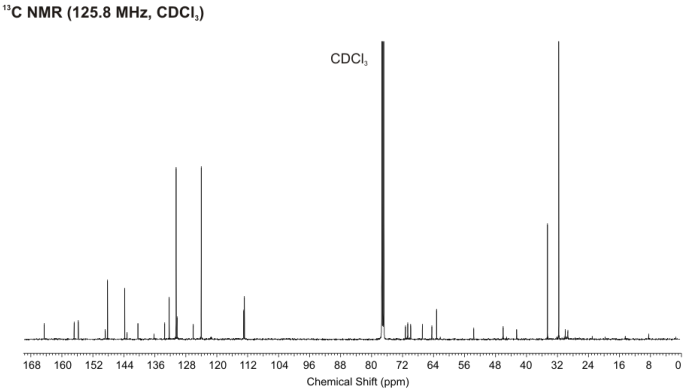

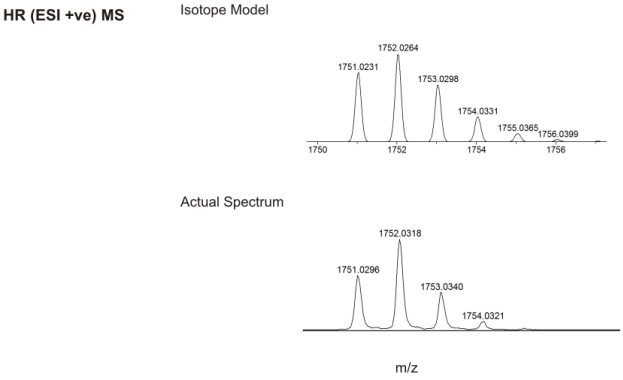

Supplementary Fig. S2 ^{1}H and ^{13}C NMR spectra and high resolution MS of rotaxane **8**·Cl.

Thread **10**·Cl

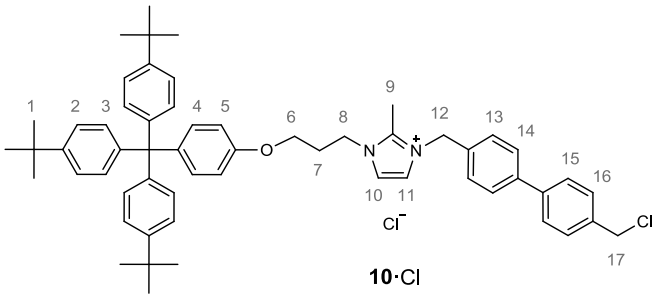

10·Cl

^{1}**H NMR (300 MHz, CDCl$_3$)**

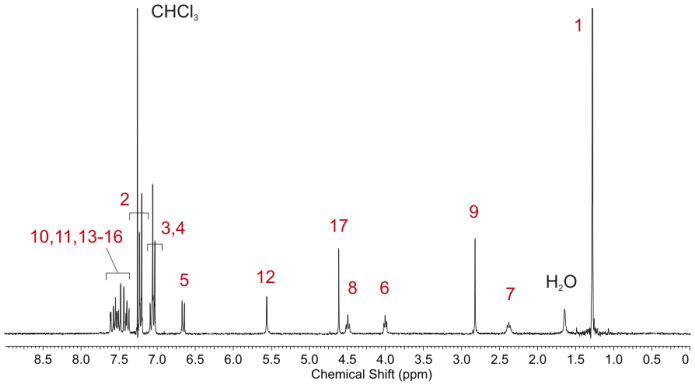

^{13}**C NMR (75.5 MHz, CDCl$_3$)**

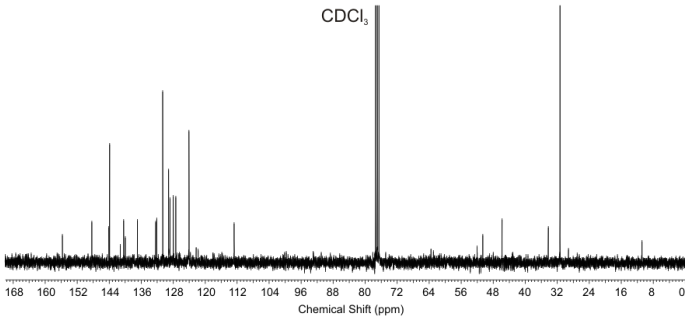

HR (ESI +ve) MS

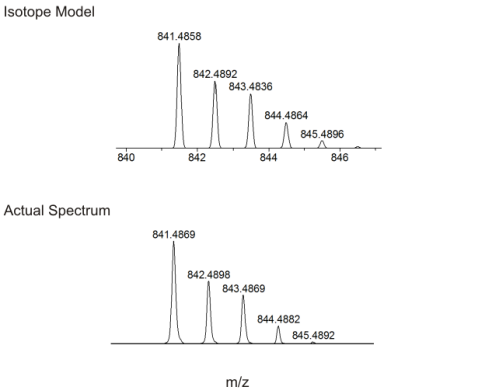

Supplementary Fig. S3 ^{1}H and ^{13}C NMR spectra and high resolution MS of thread **10**·Cl.

Thread **11**·Cl

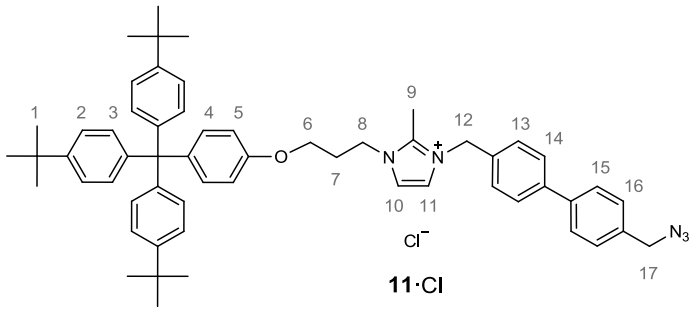

11·Cl

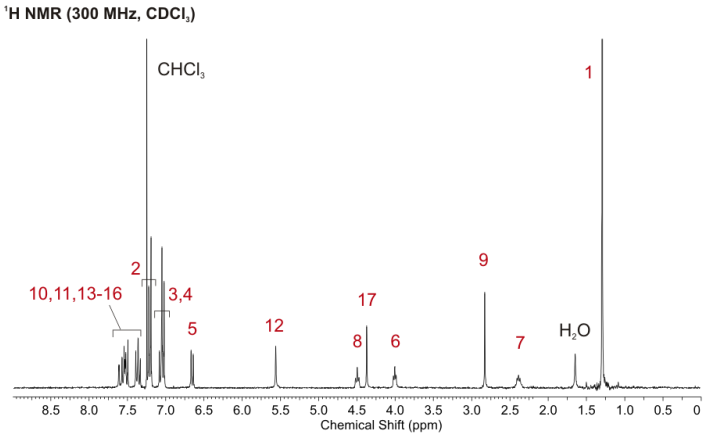

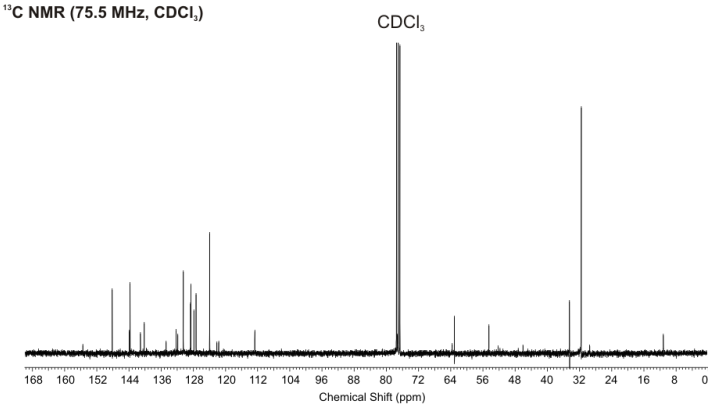

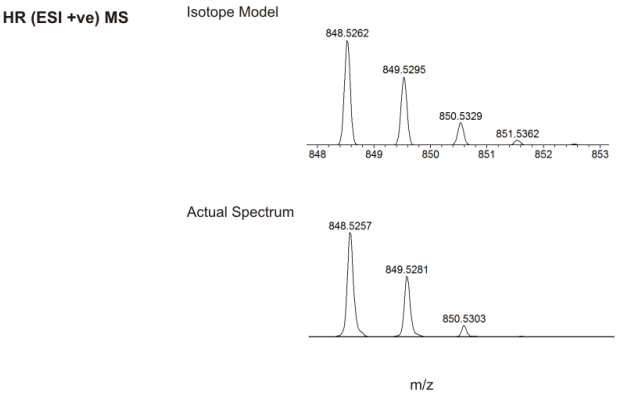

Supplementary Fig. S4 ^{1}H and ^{13}C NMR spectra and high resolution MS of thread **11**·Cl.

Rotaxane **13**·PF_6

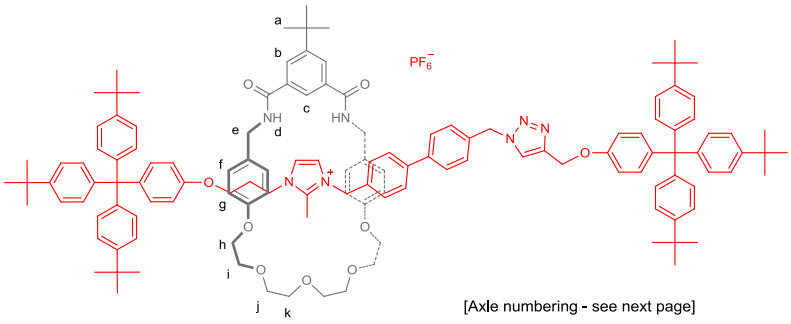

13·PF_6

^{1}H NMR (500 MHz, $CDCl_3$)

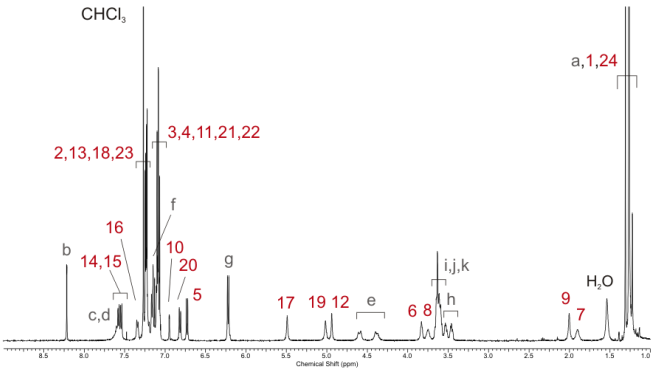

^{13}C NMR (125.8 MHz, $CDCl_3$)

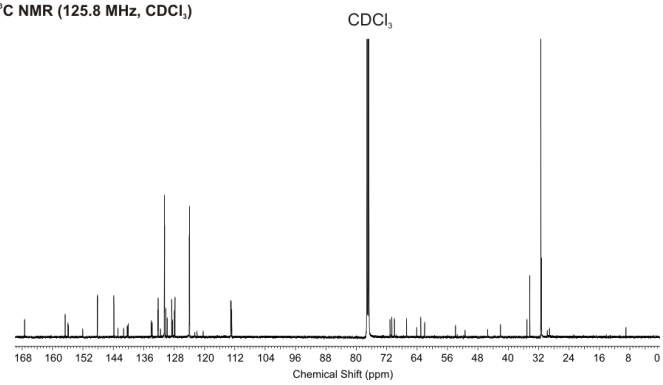

HR (ESI +ve) MS

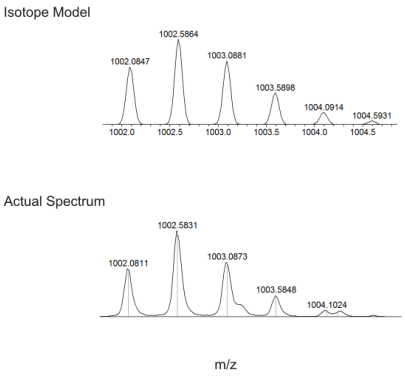

Supplementary Fig. S5 ^{1}H and ^{13}C NMR spectra and high resolution MS of rotaxane **13**·PF_6.

Axle **14**·PF_6

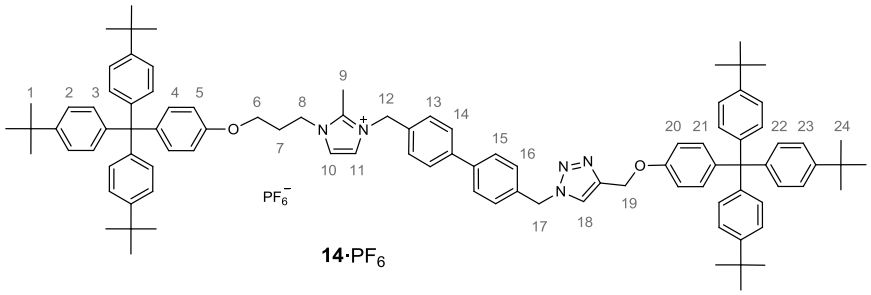

^{1}H NMR (500 MHz, $CDCl_3$)

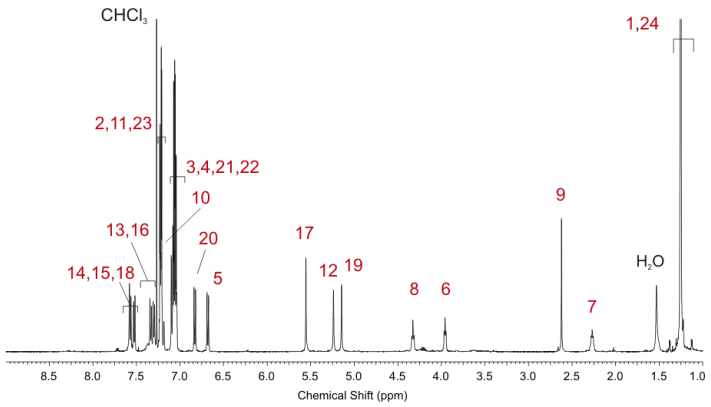

^{13}C NMR (75.5 MHz, $CDCl_3$)

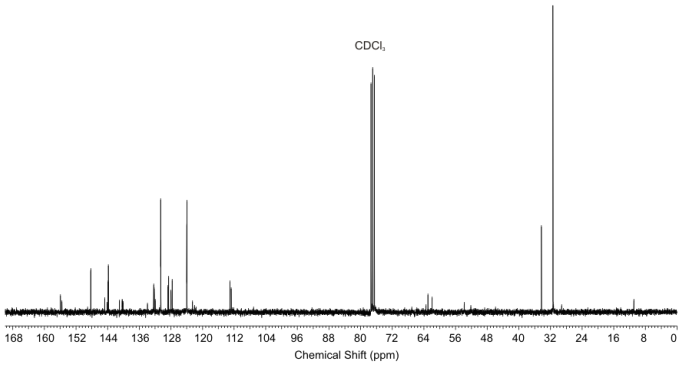

HR (ESI +ve) MS

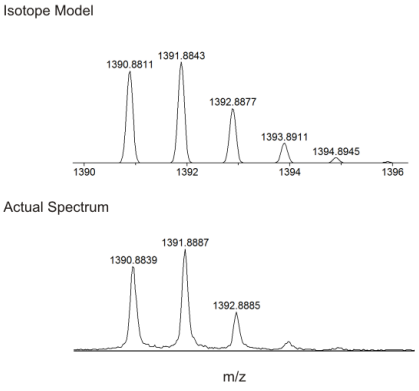

Supplementary Fig. S6 ^{1}H and ^{13}C NMR spectra and high resolution MS of axle **14**·PF_6.

Part II: ^{1}H-^{1}H 2D ROESY NMR Spectra

Pseudorotaxane **1**·**4**·Cl

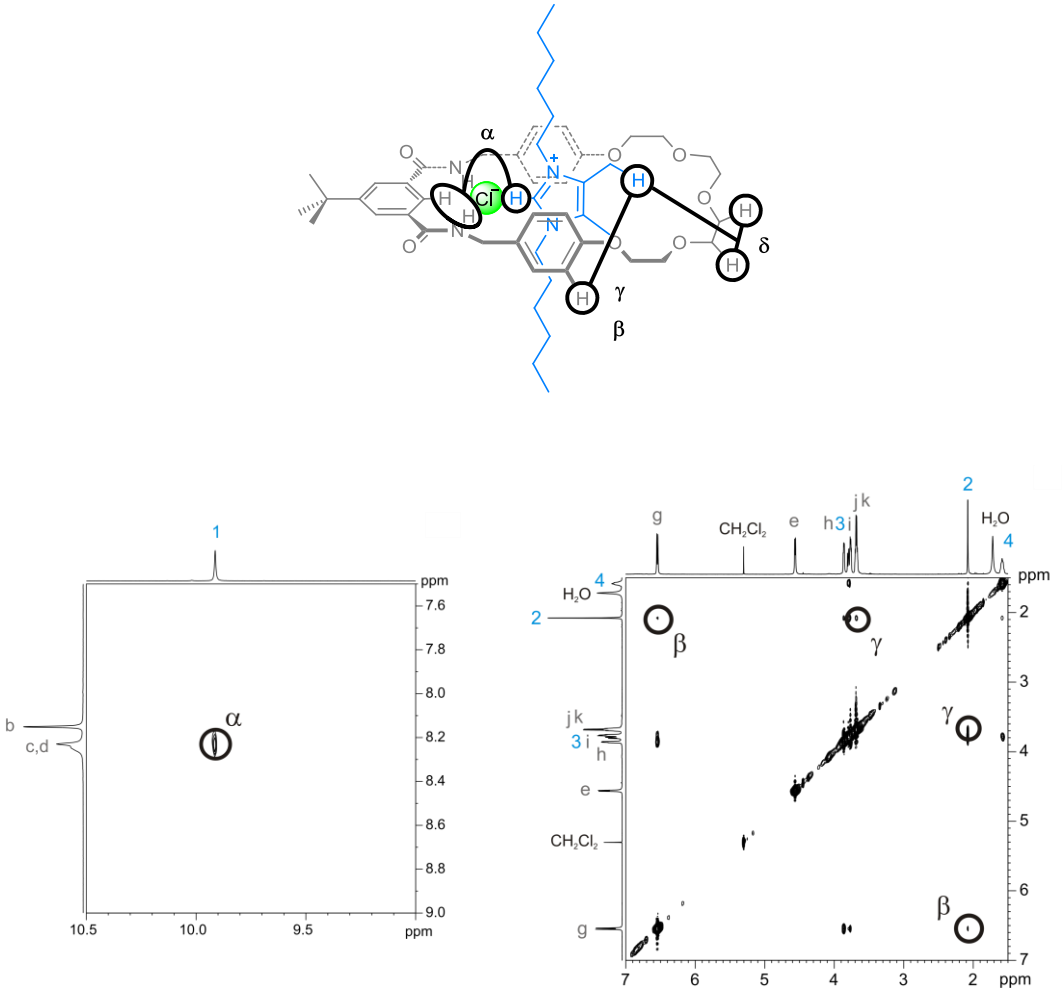

Supplementary Fig. S7 Portion of the ^{1}H-^{1}H ROESY spectrum of **1**·**4**·Cl ($CDCl_3$, 500 MHz, 293 K). Intercomponent correlations are marked on the structure.

Pseudorotaxane **2**·**4**·Cl

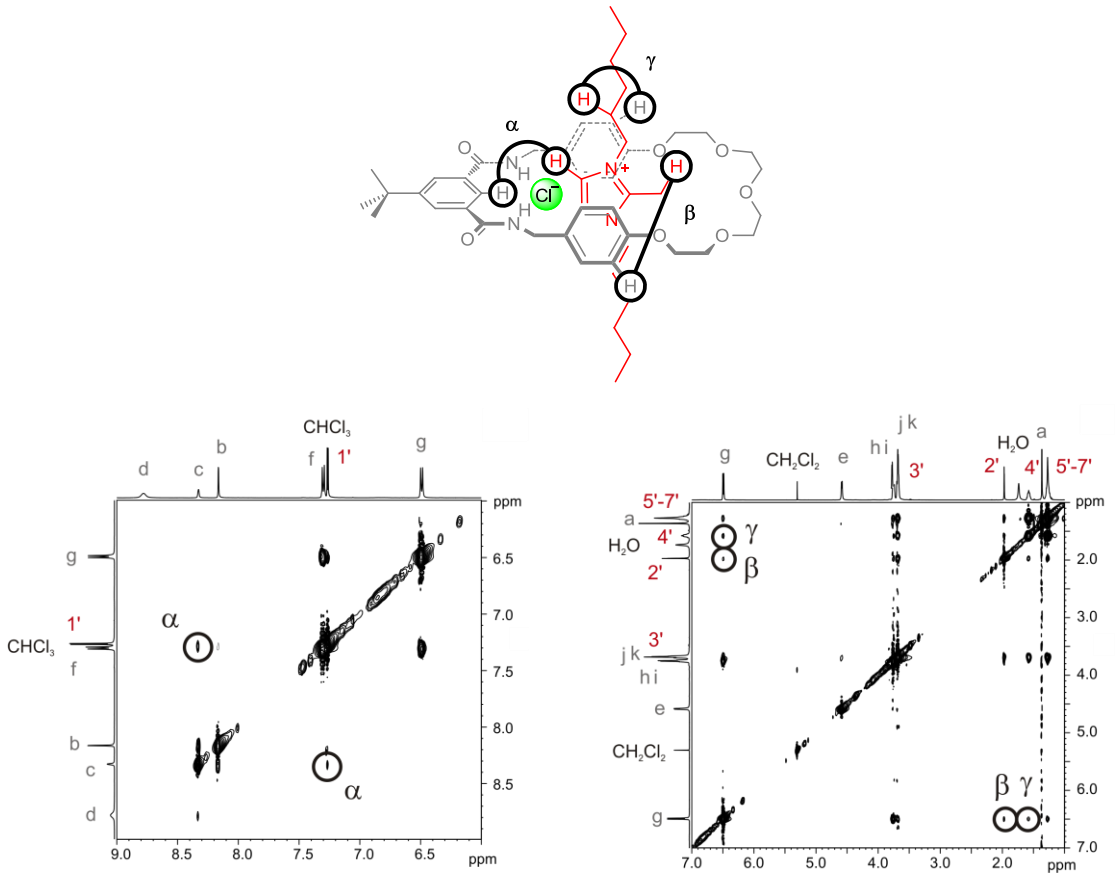

Supplementary Fig. S8 Portions of the ^{1}H-^{1}H ROESY spectrum of **2**·**4**·Cl ($CDCl_3$, 500 MHz, 293 K). Intercomponent correlations are marked on the structure.

Rotaxane **8**·Cl

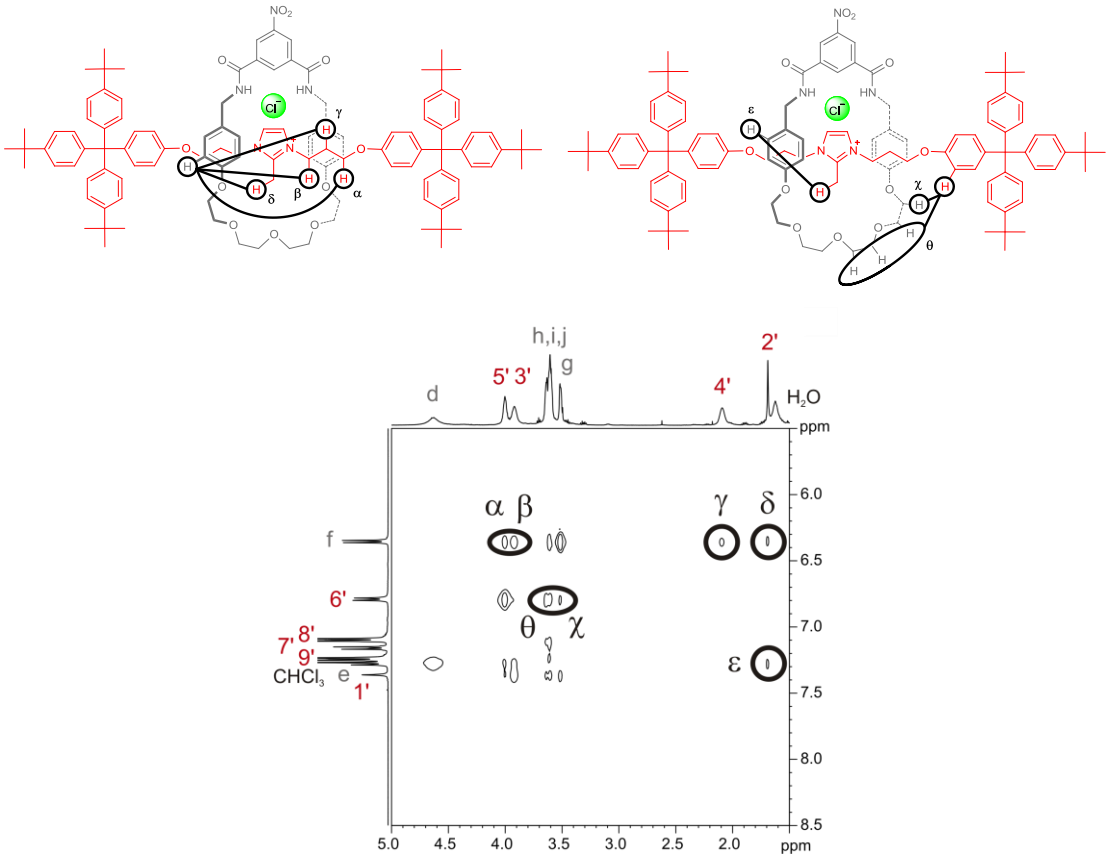

Supplementary Fig. S9 Portion of the ^{1}H-^{1}H ROESY spectrum of **8**·Cl ($CDCl_3$, 500 MHz, 293 K). Intercomponent correlations are marked on the structures.

Rotaxane **13**·PF_6

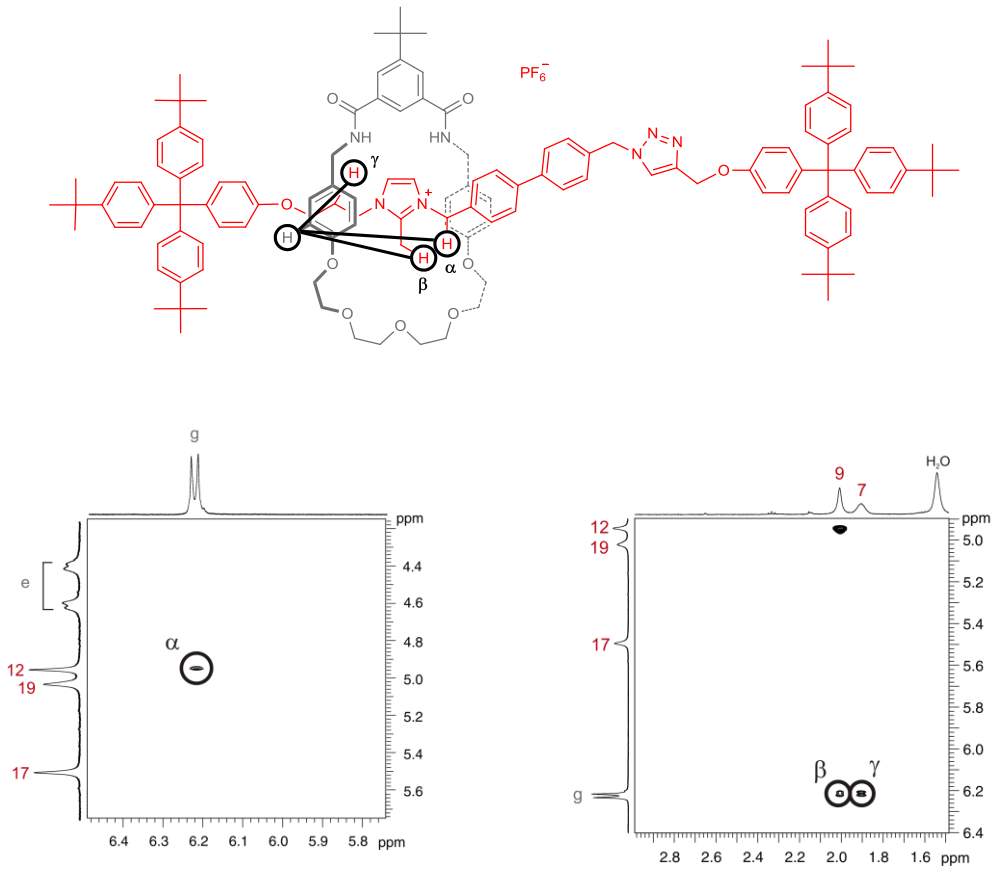

Supplementary Fig. S10 Portions of the ^{1}H-^{1}H ROESY spectrum of **13**·PF_6 ($CDCl_3$, 500 MHz, 293 K). Intercomponent correlations are marked on the structure.

Part III: ^{1}H NMR Titrations

Protocols

All ^{1}H NMR titrations were conducted at 293 K with the spectra recorded on a Varian Unity Plus 500 spectrometer.

Pseudorotaxane Titrations:
To a 0.50 ml, 2.0 x 10^{-3} M solution of the macrocycle (**4** or **5**) were added aliquots of the thread (**1**·Cl, **2**·Cl, **1**·PF_6 or **2**·PF_6) such that spectra were recorded at 0.2, 0.4, 0.6, 0.8, 1.0, 1.2, 1.4, 1.6, 1.8, 2.0, 2.5, 3.0, 4.0, 5.0, 7.0, 10.0 equivalents, with a total of 100μl added. The macrocycle amide protons (d) were monitored throughout the titrations and association constants were obtained by WinEQNMR2 analysis.

Macrocycle TBACl Titrations:
To a 0.50 ml, 2.0 x 10^{-3} M solution of the host (macrocycle **4** or **5**) were added aliquots of TBACl such that spectra were recorded at 0.2, 0.4, 0.6, 0.8, 1.0, 1.2, 1.4, 1.6, 1.8, 2.0, 2.5, 3.0, 4.0, 5.0, 7.0, 10.0 equivalents, with a total of 100μl added. The macrocycle amide protons (d) were monitored throughout the titrations and association constants were obtained by WinEQNMR2 analysis.

Rotaxane **13**·PF_6:
To a 0.50 ml, 1.5 x 10^{-3} M solution of the host were added aliquots of the guests such that spectra were recorded at 0.2, 0.4, 0.6, 0.8, 1.0, 1.2, 1.4, 1.6, 1.8, 2.0, 2.5, 3.0, 4.0, 5.0, 7.0, 10.0 equivalents, with a total of 100μl added. The para-isophthalamide proton (c) was monitored throughout the titrations, and association constants obtained by WinEQNMR2 analysis.

WinEQNMR2[1]:
The titration data were analysed initially using approximations of Job plots to confirm the binding stoichiometries.[2]
Association constants were then obtained using WinEQNMR2[1] computer programme as the associations were found to be fast on the NMR timescale. The values of the observed chemical shift in the monitored proton signal and the species concentrations were entered for every titration point and estimates for the binding constant and limiting chemical shifts were made. The parameters were refined using non-linear least-squares analysis to obtain the best fit between observed and calculated chemical shifts for a 1:1 binding stoichiometry. The

program reveals the accuracy of the calculated binding isotherm, and the input parameters were varied until the best-fit values of the stability constants, and their errors, converged.

For ease of comparison and to provide the best indication of the accuracy of the fit, the calculated association constants and their errors are given as absolute values without any rounding, e.g. 3287 (177) M^{-1}. As a consequence, the association constants are often quoted to significant figures beyond that of their error values, and this is taken into consideration when discussing binding trends.

Pseudorotaxane Titration Curves for Macrocycle 4:

Phenolic protons f and g:

a)

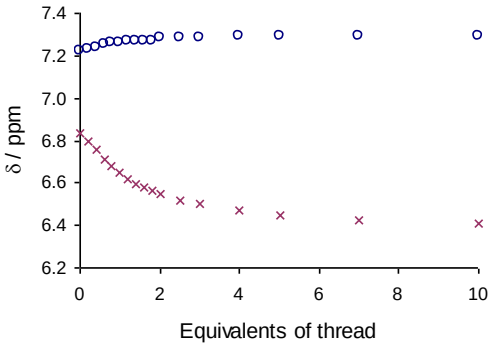

b)

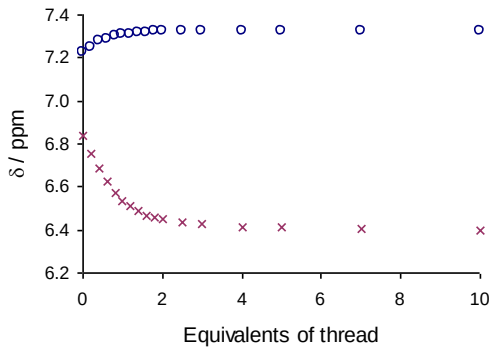

c)

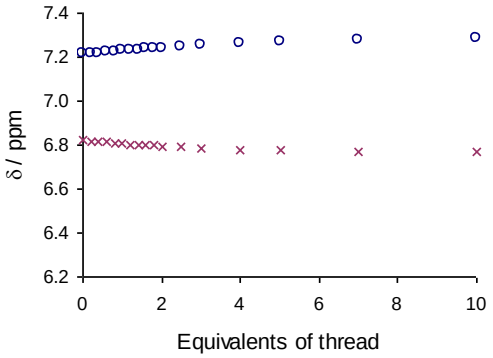

d)

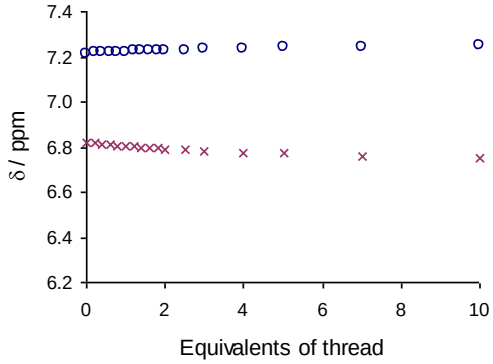

e)

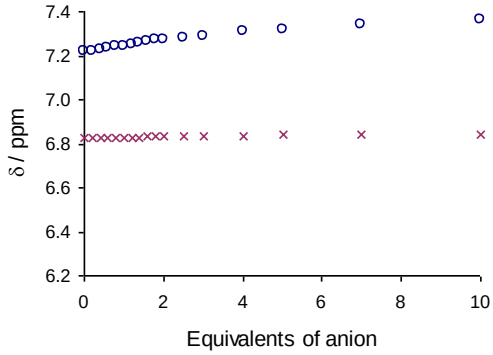

Supplementary Fig. S11 Changes in the chemical shift of phenolic protons f (o) and g (×) upon addition of a) thread **1**·Cl, b) thread **2**·Cl, c) thread **1**·PF_6, d) thread **2**·PF_6, and e) TBACl to macrocycle **4** in $CDCl_3$ at 293 K (500 MHz).

Amide protons d:

a)

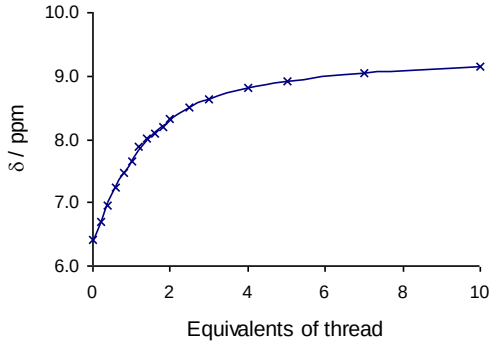

b)

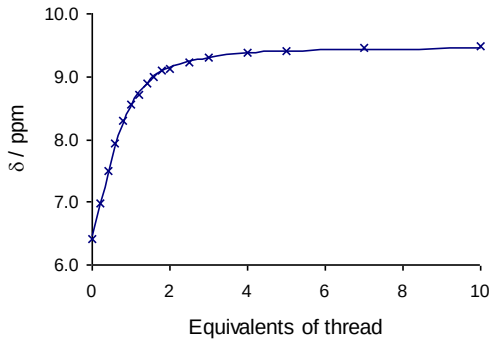

c)

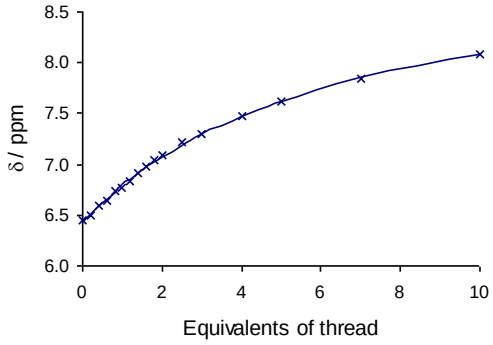

Supplementary Fig. S12 Changes in the chemical shift of amide protons d upon addition of a) thread **1**·Cl, b) thread **2**·Cl, and c) TBACl to macrocycle **4** in $CDCl_3$ at 293 K. Crosses represent experimental data points; lines represent calculated binding isotherms.

Imidazolium methyl protons 2 / 2':

a)

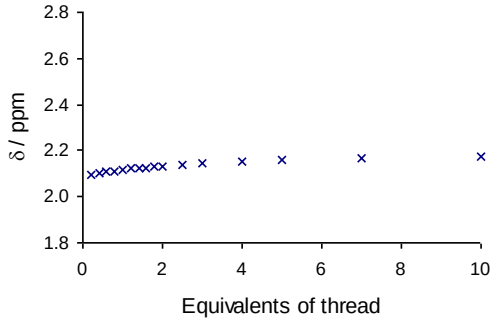

b)

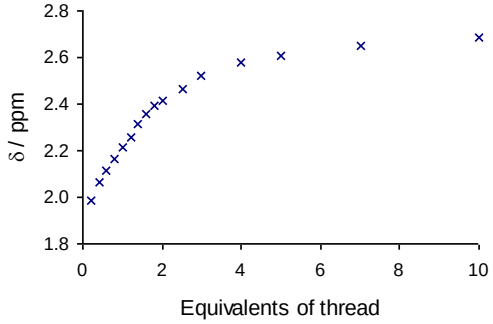

Supplementary Fig. S13 Changes in the chemical shift of imidazolium methyl protons upon addition of a) thread **1**·Cl (protons 2) and b) thread **2**·Cl (protons 2') to macrocycle **4** in $CDCl_3$ at 293 K.

Pseudorotaxane Titration Curves for Macrocycle 5:

Amide protons d:

a)

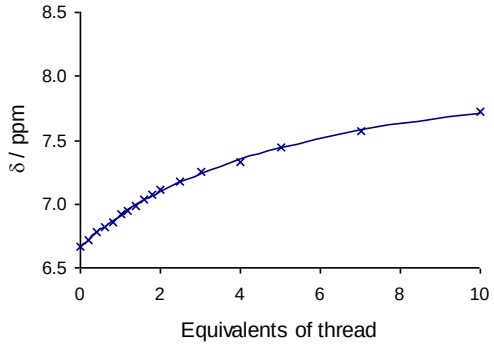

b)

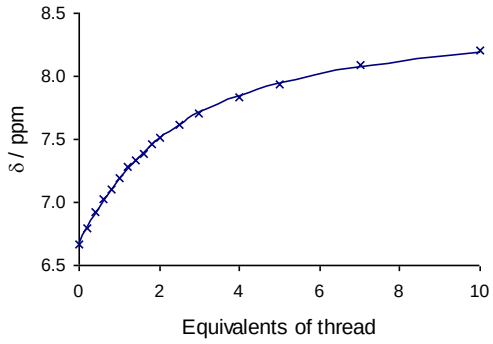

c)

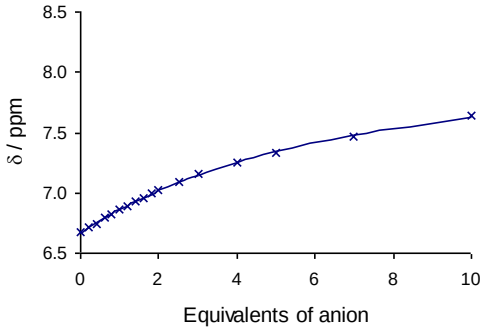

Supplementary Fig. S14 Changes in the chemical shift of amide protons d upon addition of a) thread **1**·Cl, and b) thread **2**·Cl, and c) TBACl, to macrocycle **5** in $CDCl_3$ at 293 K. Crosses represent experimental data points; lines represent calculated binding isotherms.

Imidazolium methyl protons 2 / 2':

a)

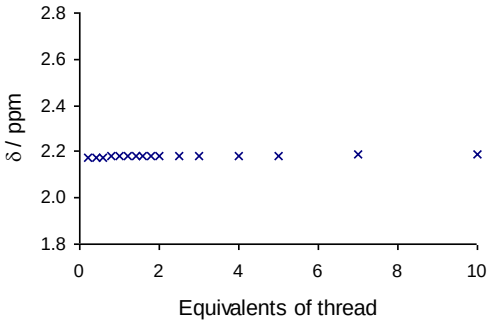

b)

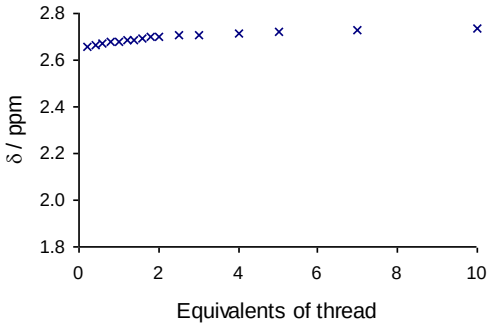

Supplementary Fig. S15 Changes in the chemical shift of imidazolium methyl protons upon addition of a) thread **1**·Cl (protons 2) and b) thread **2**·Cl (protons 2') to macrocycle **5** in $CDCl_3$ at 293 K.

Titration Curves for Rotaxane 13·PF_6:

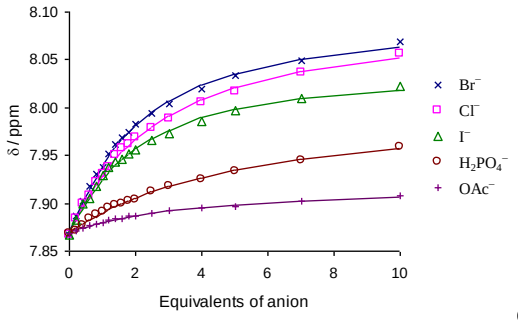

Supplementary Fig. S16 Changes in the chemical shift of para-isophthalamide proton c upon addition of anions to rotaxane **13**·PF_6 in 1:1 CD_3Cl/CD_3OD at 293 K. Symbols represent experimental data points; lines represent calculated binding isotherms.

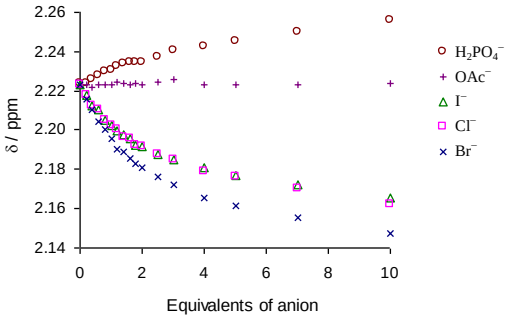

Supplementary Fig. S17 Changes in the chemical shift of imidazolium methyl protons 9 upon addition of anions to rotaxane **13**·PF_6 in 1:1 CD_3Cl/CD_3OD at 293 K.

Part IV: Discussion of Pseudorotaxane Equilibria

The multitude of equilibria occurring during the pseudorotaxane titrations are shown in Scheme S1. The titration protocol involved the addition of a thread ion pair (**1**·Cl or **2**·Cl) to a macrocycle (**3**, **4** or **5**), which is represented at the centre of Scheme S1 with the equilibrium of interest, anion templated pseudorotaxane formation, given by K_2. Whilst WinEQNMR2 analysis of the titration data determined apparent 1:1 association constants for this process, these assemblies are strictly ternary complexes. Hence, it is necessary to assess the assumption that the values reflect the relative stabilities of the anion templated pseudorotaxane assemblies.[3]

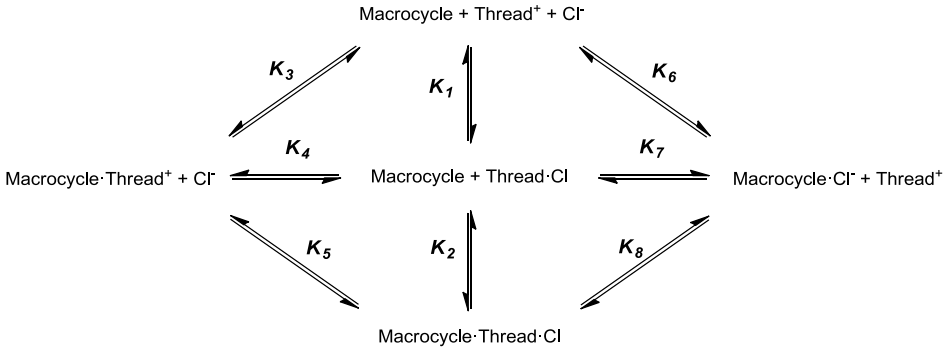

Supplementary Scheme S1 Anion templated pseudorotaxane formation equilibria.

Due to strong ion-pairing in non-competitive solvents such as $CDCl_3$, the dissociation of the thread ion pair, K_1, is considered to have a minor effect in solution and this is likely to be a valid assumption for the two imidazolium systems.

It should be noted that if ion pair dissociation did have an effect, it would be more significant for the considerably weaker binding 2-methylimidazolium motif compared with the 4,5-dimethyl analogue.[4] If so, this would result in an underestimation of K_2 for the pseudorotaxane titrations involving **2**·Cl compared with those involving **1**·Cl. Hence, while the apparent association constants for **2**·**3**·Cl, **2**·**4**·Cl and **2**·**5**·Cl were observed to be greater than those for **1**·**3**·Cl, **1**·**4**·Cl and **1**·**5**·Cl respectively (Table 1), these considerations mean that the differences in the 'true' association constants may actually be slightly larger.

As well as the thread ion pair equilibrium K_1, there are a number of other equilibria to consider, including K_3, K_4 and K_5 which represent non-anion-templated pseudorotaxane formation. The possibility of this mechanism occurring was investigated by control titrations with **1**·PF_6 and **2**·PF_6 and found to be minor compared with the anion templated process.[5] Equilibria K_6, K_7 and K_8 concern chloride binding to the macrocycle *via* abstraction from the imidazolium thread. The association constants for chloride binding to macrocycles **3**, **4** and **5** were calculated from titrations with TBA chloride to be 36(1), 82(5) and 64(3) M^{-1}

respectively (the value for **3** has been previously reported,[6] whilst the values for **4** and **5** were calculated from titrations detailed above, Fig. S12c and S14c). As these values are considerably less than the analogous binding strengths of the 4,5-dimethyl- and 2-methyl-imidazolium motifs (3044 and 782 M^{-1} respectively),[4] it can be assumed that K_6, K_7 and K_8 also have only a small effect on pseudorotaxane formation.

Hence, it was concluded that the apparent association constants calculated from the titration data can be thought to reflect the relative stabilities of the anion templated pseudorotaxane assemblies.

Part V: Crystallographic Information

Macrocycle 4

Single crystal X-ray diffraction data were collected using silicon double crystal monochromated synchrotron radiation (λ = 0.68890 Å) at Diamond Light Source beamline I19 using a custom-built Rigaku diffractometer equipped with a Cryostream N_2 open-flow cooling device.[7] The data were collected at 100(2) K via a series of ω-scans that were performed in such a way as to cover a half-sphere of data to a maximum resolution of 0.77 Å. Cell parameters and intensity data (including inter-frame scaling) were processed using CrysAlis Pro.[8]

The structures were solved by charge-flipping methods using SUPERFLIP[9] and refined using full-matrix least- squares on F^2 within the CRYSTALS suite.[10] All non-hydrogen atoms were refined with anisotropic displacement parameters. Hydrogen atoms were generally visible in the difference map and their positions and displacement parameters were refined using restraints prior to inclusion into the model using riding constraints.[11]

Both hydroquinone rings, as well as part of the polyether chain of the macrocycle are disordered. This was modelled by having two positions for all these atoms; the occupancies of the positions were refined and then fixed. Some residual electron density is present around one of the disordered hydroquinone groups – attempts to model this as a third position of the disorder were unsuccessful.

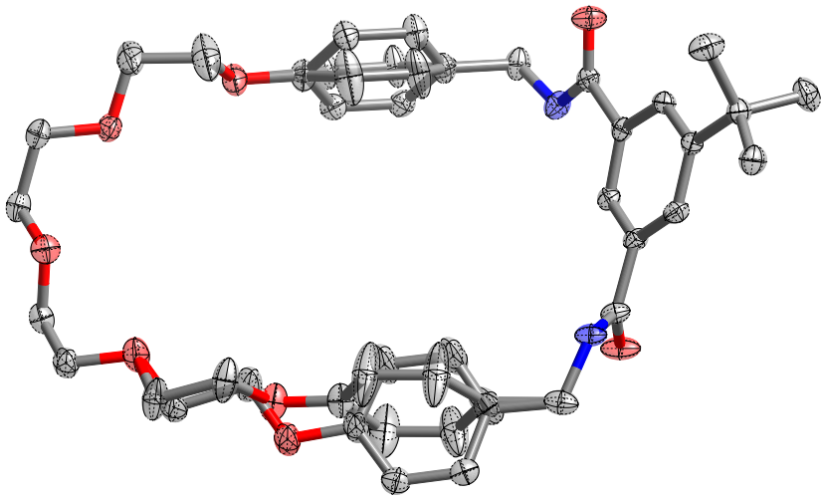

Supplementary Fig. S18 X-ray crystal structure of **4**. Thermal ellipsoids displayed at 50% probability. Hydrogen atoms omitted for clarity.

Supplementary Table S1 Selected crystallographic data for **4**

Compound reference	**4**
Chemical formula	$C_{34}H_{42}N_2O_7$
Formula Mass	590.72
Crystal system	Monoclinic
a/Å	18.3395(6)
b/Å	19.6643(5)
c/Å	8.8486(2)
α/°	90
β/°	100.766(3)
γ/°	90
Unit cell volume/Å^3	3134.93(15)
Temperature/K	100
Space group	*P*21/*c*
No. of formula units per unit cell, *Z*	4
No. of reflections measured	42173
No. of independent reflections	11113
R_{int}	0.0466
Final R_1 values ($I > 2\sigma(I)$)	0.0738
Final $wR(F^2)$ values ($I > 2\sigma(I)$)	0.1580
Final R_1 values (all data)	0.0860
Final $wR(F^2)$ values (all data)	0.1692
CCDC number	**888917**

Pseudorotaxane 2·4·**Cl**

Single crystal X-ray diffraction data for **2·4**·Cl were collected using graphite monochromated Cu Kα radiation (λ= 1.54184 Å) on an Oxford Diffraction SuperNova diffractometer. The diffractometer was equipped with a Cryostream N_2 open-flow cooling device,[7] and the data were collected at 150(2) K. Series of ω-scans were performed in such a way as to collect all unique reflections to a maximum of 0.80 Å. Cell parameters and intensity data (including inter-frame scaling) were processed using CrysAlis Pro.

The structures were solved by charge-flipping methods using SUPERFLIP[9] and refined using full-matrix least-squares on F^2 within the CRYSTALS suite.[10] All non-hydrogen atoms were refined with anisotropic displacement parameters. Hydrogen atoms were generally visible in

the difference map and their positions and displacement parameters were refined using restraints prior to inclusion into the model using riding constraints.[11]

The molecule could only be successfully solved in the non-centrosymmetric spacegroup, P1, with a Z` of 2. This suggests that a centre of inversion may be present, giving the centrosymmetric space group, with Z` = 1. Attempts to find such a smaller cell using the ADDSYM feature of PLATON were unsuccessful.[12] Inspection of the atom positions reveals that the two independent pseudorotaxanes are not in fact related by a centre of inversion, and so this structure was refined and finalised in the P1 spacegroup.

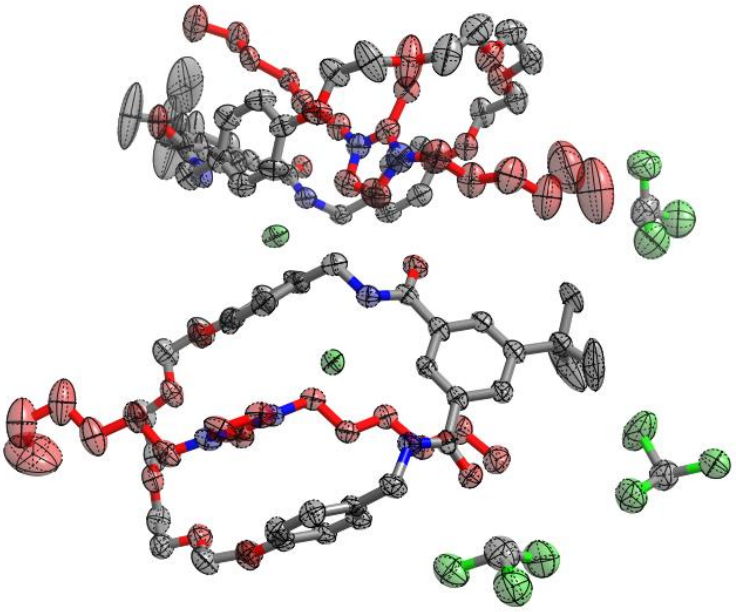

Supplementary Fig. S19 X-ray crystal structure of **2**·**4**·Cl. Thermal ellipsoids displayed at 50% probability. Hydrogen atoms omitted for clarity.

As noted in the main text, in constrast to the analogous, previously reported pseudorotaxane assembly with larger macrocycle **3** (**2**·**3**·Cl), the inter-assembly considerations appear to be much less important in the solid-state structure of **2**·**4**·Cl than the anion templation interactions within individual pseudorotaxanes. For comparison with the values given in the previous study,[4] for **2**·**4**·Cl: the halide anion in the same assembly is much closer to the centre of the imidazolium positive charge[13] than the next nearest anion, with corresponding distances of 4.928(2) or 4.978(3) Å (for the two assemblies in the asymmetric unit) compared to 6.820(2) or 7.032(3) Å.

Supplementary Table S2 Selected crystallographic data for **2·4**·Cl

Compound reference	**2·4**·Cl
Chemical formula	$C_{34}H_{42}N_2O_7 \cdot C_{16}H_{31}N_2 \cdot Cl \cdot 1.5(CHCl_3)$
Formula Mass	1056.67
Crystal system	Triclinic
a/Å	9.0382(4)
b/Å	16.6844(6)
c/Å	19.2103(12)
α/°	79.817(4)
β/°	77.978(4)
γ/°	89.217(3)
Unit cell volume/Å^3	2787.9(2)
Temperature/K	150
Space group	*P*1
No. of formula units per unit cell, *Z*	2
No. of reflections measured	28075
No. of independent reflections	13586
R_{int}	0.0504
Final R_1 values ($I > 2\sigma(I)$)	0.1155
Final $wR(F^2)$ values ($I > 2\sigma(I)$)	0.3081
Final R_1 values (all data)	0.1210
Final $wR(F^2)$ values (all data)	0.3195
CCDC number	**888918**

Part V: References

1. M. J. Hynes, *J. Chem. Soc., Dalton Trans.*, 1993, 311-312.
2. M. T. Blanda, J. H. Horner and M. Newcomb, *J. Org. Chem.*, 1989, **54**, 4626-4636.
3. M. R. Sambrook, P. D. Beer, J. A. Wisner, R. L. Paul, A. R. Cowley, F. Szemes and M. G. B. Drew, *J. Am. Chem. Soc.*, 2005, **127**, 2292-2302.
4. G. T. Spence, C. J. Serpell, J. Sardinha, P. J. Costa, V. Félix and P. D. Beer, *Chem. Eur. J.*, 2011, **17**, 12955-12966.
5. The small shifts during these titrations indicate minimal donor–acceptor interactions and prevented the calculation of any accurate association constants using WinEQNMR2.
6. C. J. Serpell, N. L. Kilah, P. J. Costa, V. Félix and P. D. Beer, *Angew. Chem. Int. Ed.*, 2010, **49**, 5322-5326.
7. J. Cosier and A. M. Glazer, *J. Appl. Crystallogr.*, 1986, **19**, 105-107.
8. CrysAlis Pro, Oxford Diffraction (2011).
9. L. Palatinus and G. Chapuis, *J. Appl. Crystallogr.*, 2007, **40**, 786-790.
10. P. W. Betteridge, J. R. Carruthers, R. I. Cooper, K. Prout and D. J. Watkin, *J. Appl. Crystallogr.*, 2003, **36**, 1487.
11. R. I. Cooper, A. L. Thompson and D. J. Watkin, *J. Appl. Crystallogr.*, 2010, **43**, 1100-1107.
12. A. Spek, *J. Appl. Crystallogr.*, 2003, **36**, 7-13.
13. S. Tsuzuki, H. Tokuda and M. Mikami, *Phys. Chem. Chem. Phys.*, 2007, **9**, 4780-4784.